

Technical University of Denmark



Statistical properties of kinetic and total energy densities in reverberant spaces

Jacobsen, Finn; Molares, Alfonso Rodriguez

Published in:
Acoustical Society of America. Journal

Link to article, DOI:
[10.1121/1.3304158](https://doi.org/10.1121/1.3304158)

Publication date:
2010

Document Version
Publisher's PDF, also known as Version of record

[Link back to DTU Orbit](#)

Citation (APA):
Jacobsen, F., & Molares, A. R. (2010). Statistical properties of kinetic and total energy densities in reverberant spaces. *Acoustical Society of America. Journal*, 127(4), 2332-2337. DOI: 10.1121/1.3304158

DTU Library

Technical Information Center of Denmark

General rights

Copyright and moral rights for the publications made accessible in the public portal are retained by the authors and/or other copyright owners and it is a condition of accessing publications that users recognise and abide by the legal requirements associated with these rights.

- Users may download and print one copy of any publication from the public portal for the purpose of private study or research.
- You may not further distribute the material or use it for any profit-making activity or commercial gain
- You may freely distribute the URL identifying the publication in the public portal

If you believe that this document breaches copyright please contact us providing details, and we will remove access to the work immediately and investigate your claim.

Statistical properties of kinetic and total energy densities in reverberant spaces^{a)}

Finn Jacobsen^{b)}

Department of Electrical Engineering, Acoustic Technology, Technical University of Denmark, Building 352, DK-2800 Kongens Lyngby, Denmark

Alfonso Rodríguez Molares

E.T.S.E. Telecomunicación, Universidade de Vigo, Campus Lagoas-Marcosende, E-36310 Vigo, Spain

(Received 16 July 2009; revised 7 January 2010; accepted 8 January 2010)

Many acoustical measurements, e.g., measurement of sound power and transmission loss, rely on determining the total sound energy in a reverberation room. The total energy is usually approximated by measuring the mean-square pressure (i.e., the potential energy density) at a number of discrete positions. The idea of measuring the total energy density instead of the potential energy density on the assumption that the former quantity varies less with position than the latter goes back to the 1930s. However, the phenomenon was not analyzed until the late 1970s and then only for the region of high modal overlap, and this analysis has never been published. Moreover, until fairly recently, measurement of the total sound energy density required an elaborate experimental arrangement based on finite-difference approximations using at least four amplitude and phase matched pressure microphones. With the advent of a three-dimensional particle velocity transducer, it has become somewhat easier to measure total rather than only potential energy density in a sound field. This paper examines the ensemble statistics of kinetic and total sound energy densities in reverberant enclosures theoretically, experimentally, and numerically.

© 2010 Acoustical Society of America. [DOI: 10.1121/1.3304158]

PACS number(s): 43.55.Cs, 43.58.Bh [AJZ]

Pages: 2332–2337

I. INTRODUCTION

Many acoustical measurements rely on determining the sound energy in an enclosure. Examples include standardized measurements of sound power and transmission loss in reverberation rooms. The total sound energy is usually estimated by measuring the mean-square pressure (that is, the potential energy density) either at a number of discrete positions or using a moving microphone, and much effort has been spent on developing efficient averaging procedures.^{1,2} The idea of measuring the total energy density rather than the potential energy density on the assumption that the former quantity varies less with position than the latter goes back to the 1930s and has occasionally been discussed in the literature.^{3,4} In the late 1970s the phenomenon was analyzed using a stochastic interference model of a diffuse sound field,⁵ and in the late 1980s the matter was examined experimentally for the first time.⁶ However, until recently measurement of the total sound energy density has required an elaborate arrangement based on finite-difference approximations using at least four pressure microphones.^{6–9} The microphones should be amplitude and phase matched very well,

and the signal-to-noise ratio is poor because the finite-difference signals should be time integrated,¹⁰ which is perhaps one of the reasons why the method has not been used much in practice. With the advent of a three-dimensional particle velocity transducer, “Microflown,”¹¹ it has become somewhat easier to measure kinetic and total rather than only potential energy density in a sound field, as demonstrated a few years ago.¹²

A recent investigation examined the ensemble statistics of the sound power emitted by a monopole in reverberant surroundings using Waterhouse’s random wave theory¹³ extended to the region of low modal overlap.¹⁴ Another recent investigation used the same model to examine the ensemble statistics of potential energy density.¹⁵ The purpose of the present study is to examine the ensemble statistics of kinetic and total sound energy densities in reverberant spaces theoretically, experimentally, and numerically.

II. THE RANDOM WAVE THEORY

A. The region of high modal overlap

The starting point of this investigation is a stochastic pure-tone diffuse-field interference model of the sound field in a reverberation room originally developed by Waterhouse.¹³ This model describes the sound field as a sum of plane waves arriving with random phase angles from random directions,

^{a)} Portions of this work were presented in “Measurement of total sound energy in an enclosure at low frequencies,” Proceedings of Acoustics ’08, Paris, France, July 2008, pp. 3249–3254, and “The uncertainty of pure tone measurements in reverberation rooms below the Schroeder frequency,” Proceedings of Sixteenth International Congress on Sound and Vibration, Krakow, Poland, July 2009.

^{b)} Author to whom correspondence should be addressed. Electronic mail: fja@elektro.dtu.dk

$$p(\mathbf{r}) = \lim_{N \rightarrow \infty} \frac{1}{\sqrt{N}} \sum_{n=1}^N A_n e^{j(\omega t - \mathbf{k}_n \cdot \mathbf{r})}, \quad (1)$$

where $p(\mathbf{r})$ is the sound pressure at position \mathbf{r} , A_n is a complex random amplitude the phase angle of which is uniformly distributed between 0 and 2π , and \mathbf{k}_n is a random wave number vector with a uniform distribution over all directions. The corresponding particle velocity components in three perpendicular directions can be written as

$$u_x(\mathbf{r}) = \lim_{N \rightarrow \infty} \frac{1}{\sqrt{N}} \sum_{n=1}^N \frac{A_n \sin \theta_n \cos \varphi_n}{\rho c} e^{j(\omega t - \mathbf{k}_n \cdot \mathbf{r})}, \quad (2a)$$

$$u_y(\mathbf{r}) = \lim_{N \rightarrow \infty} \frac{1}{\sqrt{N}} \sum_{n=1}^N \frac{A_n \sin \theta_n \sin \varphi_n}{\rho c} e^{j(\omega t - \mathbf{k}_n \cdot \mathbf{r})}, \quad (2b)$$

$$u_z(\mathbf{r}) = \lim_{N \rightarrow \infty} \frac{1}{\sqrt{N}} \sum_{n=1}^N \frac{A_n \cos \theta_n}{\rho c} e^{j(\omega t - \mathbf{k}_n \cdot \mathbf{r})}, \quad (2c)$$

where φ_n and θ_n are the azimuth and polar angles defining the wave number vector of the n th wave, and ρc is the characteristic impedance of air.⁵ Each set of random amplitudes and wave number vectors corresponds to an outcome of a stochastic process, and above the Schroeder frequency there is no difference between the statistics with respect to position and the full ensemble statistics.^{5,14} It is easy to show that the mean-square values of the pressure and each component of the particle velocity can be expressed as a sum of two independent squared Gaussian variables (random sums) with zero mean.^{5,13} Thus, the mean-square pressure as well as the mean-square value of any individual component of the particle velocity have a chi-square distribution with two degrees of freedom (also known as the exponential distribution),^{13,16} from which it follows that their relative (normalized) ensemble variance is 1. (The relative variance of a stochastic variable X , $\varepsilon^2\{X\}$, is the squared ratio of its standard deviation $\sigma\{X\}$ to its expected value $E\{X\}$.) Moreover, these four random variables can be shown to be statistically independent.⁵ This combined with the fact that the variance of a sum of independent random variables equals the sum of their variances¹⁶ leads to the conclusion that the relative variance of the kinetic energy density is

$$\varepsilon^2\{w_{\text{kin}}\} = \frac{\sigma^2\{w_{\text{kin},x} + w_{\text{kin},y} + w_{\text{kin},z}\}}{(E\{w_{\text{kin},x} + w_{\text{kin},y} + w_{\text{kin},z}\})^2} = \frac{3\sigma^2\{w_{\text{kin},x}\}}{9E^2\{w_{\text{kin},x}\}} = \frac{1}{3}, \quad (3)$$

where $w_{\text{kin},x}$, $w_{\text{kin},y}$, and $w_{\text{kin},z}$ are the kinetic densities corresponding to the particle velocity components associated with the x -, y -, and z -directions. Since the ensemble average of the potential energy density must equal the ensemble average of the kinetic energy density, the relative variance of the total energy density becomes

$$\begin{aligned} \varepsilon^2\{w_{\text{tot}}\} &= \frac{\sigma^2\{w_{\text{pot}} + w_{\text{kin}}\}}{(E\{w_{\text{pot}} + w_{\text{kin}}\})^2} = \frac{\sigma^2\{w_{\text{pot}}\} + \sigma^2\{w_{\text{kin}}\}}{4E^2\{w_{\text{pot}}\}} \\ &= \frac{1 + \frac{1}{3}}{4} = \frac{1}{3}. \end{aligned} \quad (4)$$

To summarize, in the region of high modal overlap, measuring the kinetic sound energy density at one position in a reverberation room gives the same statistical information as measuring the potential energy density at three statistically independent positions. No further gain is obtained by measuring the total energy density. These results have been validated experimentally⁶ and, more recently, also confirmed by a numerical implementation of the Green's function in a room.¹²

B. The region below the Schroeder frequency

When the modal overlap cannot be assumed to be high, the source that generates the sound field can no longer be assumed to emit its free field sound power.¹⁴ The reason is that the radiation impedance is affected by the random reverberant part of the sound field, which moreover is increased at the source position because of coherent backscattering or "weak Anderson localization" as predicted by Weaver and Burkhart.¹⁷ Besides, one can no longer expect the same statistics with respect to position as would be found in an ensemble of rooms.^{14,15} The resulting relative ensemble variance of the sound power emitted by a monopole has been found, based on Eq. (1), to be

$$\varepsilon^2\{P_a\} = \frac{2}{M_s}, \quad (5)$$

where M_s is the statistical modal overlap of the room.¹⁴ This quantity is the product of the modal density and the statistical modal bandwidth) and can be written as

$$M_s = \frac{12\pi \ln(10) V f^2}{T_{60} c^3} = \frac{\pi A f^2}{2c^2}, \quad (6)$$

where V is the volume of the room, T_{60} is its reverberation time, A is the total absorption area of the room, f is the frequency, and c is the speed of sound. A very different modal model based on an assumption of the modal frequencies being distributed according to the random matrix theory of Gaussian orthogonal ensembles leads to almost the same expression.¹⁸

Since the average of the squared amplitudes of the waves that compose the sound field at any frequency and in any room is proportional to the sound power emitted by the source that generates the sound field, it follows that one may expect additional ensemble variations in the kinetic and total energy densities when the modal overlap is low. Such additional variations, reflected in an increase in the relative ensemble variance, have recently been demonstrated for potential energy density.¹⁵ Moreover, because these additional variations affect the pressure and the three perpendicular particle velocity components in the same way, these components

can no longer be assumed to be statistically independent, nor can kinetic and potential energy densities be expected to be statistically independent.

One can model the phenomenon by multiplying each of the original independent exponentially distributed variables in Eqs. (3) and (4) by another random variable that represents the relative variations in the emitted sound power,

$$1 + W = \frac{P_a}{E\{P_{af}\}}. \quad (7)$$

The new variable W is normally distributed and has zero mean and a variance given by Eq. (5). It is statistically independent of the other quantities because the variations in the sound power depends only on the reverberant part of the sound pressure at the source position.¹⁴ The relative ensemble variance of the mean-square particle velocity component in an arbitrary direction now becomes

$$\begin{aligned} \varepsilon^2\{w'_{kin,x}\} &= \frac{E\{w_{kin,x}^2(1+W)^2\}}{(E\{w_{kin,x}(1+W)\})^2} - 1 \\ &= \frac{E\{w_{kin,x}^2\}E\{(1+W)^2\}}{E^2\{w_{kin,x}\}E^2\{1+W\}} - 1 \\ &= \frac{2E^2\{w_{kin,x}\}E\{(1+W)^2\}}{E^2\{w_{kin,x}\}E^2\{1+W\}} - 1 \\ &= 2(1 + E\{W^2\}) - 1 = 2\left(1 + \frac{2}{M_s}\right) - 1 = 1 + \frac{4}{M_s}, \quad (8) \end{aligned}$$

where $w'_{kin,x}$ is the modified kinetic energy density associated with the x -direction. [The first step in Eq. (8) follows from the general relation $\varepsilon^2\{X\} = E\{X^2\}/E^2\{X\} - 1$, the second step follows because the variables are statistically independent, and the third step follows from the fact that the relative variance of $w_{kin,x}$ is unity.] This expression is identical with the relative ensemble variance of potential energy density,¹⁵

$$\varepsilon^2\{w'_{pot}\} = 1 + \frac{4}{M_s}. \quad (9)$$

(The modal model mentioned above leads to a very similar expression.¹⁸) In the same way, Eq. (3) becomes

$$\begin{aligned} \varepsilon^2\{w'_{kin}\} &= \frac{E\{(w_{kin,x} + w_{kin,y} + w_{kin,z})^2(1+W)^2\}}{(E\{(w_{kin,x} + w_{kin,y} + w_{kin,z})(1+W)\})^2} - 1 \\ &= \frac{E\{(w_{kin,x} + w_{kin,y} + w_{kin,z})^2\}E\{(1+W)^2\}}{(3E\{w_{kin,x}\})^2E^2\{(1+W)\}} - 1 \\ &= \frac{3E\{w_{kin,x}^2\} + 6E^2\{w_{kin,x}\}}{9E^2\{w_{kin,x}\}}(1 + E\{W^2\}) - 1 \\ &= \frac{12E^2\{w_{kin,x}\}}{9E^2\{w_{kin,x}\}}\left(1 + \frac{2}{M_s}\right) - 1 = \frac{1}{3} + \frac{8}{3M_s}, \quad (10) \end{aligned}$$

where w'_{kin} is the modified kinetic energy density.

It is apparent that the relative variance of the modified kinetic energy density is not simply one-third of the relative variance of a single component, given by Eq. (8); it is somewhat larger. The explanation is that the modified components are no longer independent. An alternative derivation of Eq. (10) could be based on the covariance between the three modified components of the kinetic energy density.

Note that

$$\frac{\varepsilon^2\{w'_{pot}\}}{\varepsilon^2\{w'_{kin}\}} = \frac{1 + \frac{4}{M_s}}{\frac{1}{3} + \frac{8}{3M_s}} = 3 \frac{1 + \frac{4}{M_s}}{1 + \frac{8}{M_s}} \rightarrow \begin{cases} 3 & \text{for } M_s \rightarrow \infty \\ \frac{3}{2} & \text{for } M_s \rightarrow 0, \end{cases} \quad (11)$$

which shows that the statistical advantage of determining kinetic rather than potential energy density is halved at low modal overlap because of the correlation between the three particle velocity components due to the varying sound power.

Equation (4) can be modified in the same manner,

$$\begin{aligned} \varepsilon^2\{w'_{tot}\} &= \frac{E\{(w_{kin,x} + w_{kin,y} + w_{kin,z} + w_{pot})^2(1+W)^2\}}{(E\{(w_{kin,x} + w_{kin,y} + w_{kin,z} + w_{pot})(1+W)\})^2} - 1 \\ &= \frac{3E\{w_{kin,x}^2\} + 6E^2\{w_{kin,x}\} + E\{w_{pot}^2\} + 6E\{w_{pot}\}E\{w_{kin,x}\}}{4E^2\{w_{pot}\}}(1 + E\{W^2\}) - 1 \\ &= \frac{12E^2\{w_{kin,x}\} + 2E^2\{w_{pot}\} + 6E\{w_{pot}\}E\{w_{kin,x}\}}{4E^2\{w_{pot}\}}\left(1 + \frac{2}{M_s}\right) - 1 \\ &= \frac{\frac{12}{9} + 2 + \frac{6}{3}}{4}\left(1 + \frac{2}{M_s}\right) - 1 = \frac{1}{3} + \frac{8}{3M_s}. \quad (12) \end{aligned}$$

Apparently, there is no statistical advantage in measuring total rather than kinetic energy density in the region of low modal overlap either.

To summarize, the stochastic model derived in the foregoing is based on the fundamental assumption that Eq. (1) is also valid in the region of low modal overlap, although there

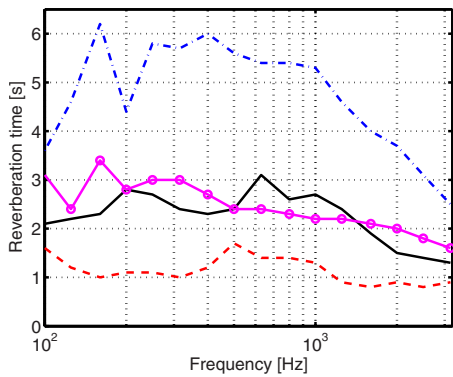


FIG. 1. (Color online) Reverberation time of the test rooms. Solid line: small lightly damped room; dashed line: small damped room; dash-dotted line: large reverberation room; line with circle markers: large damped reverberation room.

are additional variations in the random set of squared wave amplitudes, $|A_n|^2$, caused by the variations in the sound power emitted by the source. It is worth noting that in this frequency range the spatial statistics in any room depend strongly on whether the frequency is coinciding with a modal frequency or not. Equations (5), (8)–(10), and (12) express the relative variances associated with an ensemble of rooms with slightly different dimensions but the same modal overlap.

III. EXPERIMENTAL RESULTS

Some experiments have been carried out in various rooms at the Technical University of Denmark in order to validate the foregoing stochastic considerations: a small (40 m^3) lightly damped room, the same room with extra absorption, a large (245 m^3) reverberation room, and the same large room with added absorption. The reverberation times of the four rooms are shown in Fig. 1. The corresponding Schroeder frequencies are 500, 330, 310, and 200 Hz, respectively. All rooms are essentially rectangular although there are large stationary diffusers in the reverberation room.

The rooms were driven with a Brüel & Kjær (B&K) “OmniSource” (a loudspeaker) fitted with a B&K “Volume velocity adapter,” a device with two matched quarter-inch microphones for measuring the output volume velocity and sound power. Kinetic, potential, and total energy densities were measured at a number of positions using an “Ultimate sound probe” (USP), a three-dimensional pressure-velocity probe produced by Microflown (Zevenaar, The Netherlands). The three particle velocity channels were calibrated as described in Ref. 19. The frequency responses between the volume velocity of the source and the sound pressure and three perpendicular components of the particle velocity were measured with a B&K “PULSE” analyzer using pseudorandom noise (6400 spectral lines) synchronized to the analysis in the frequency range up to 3.2 kHz. The experimental technique

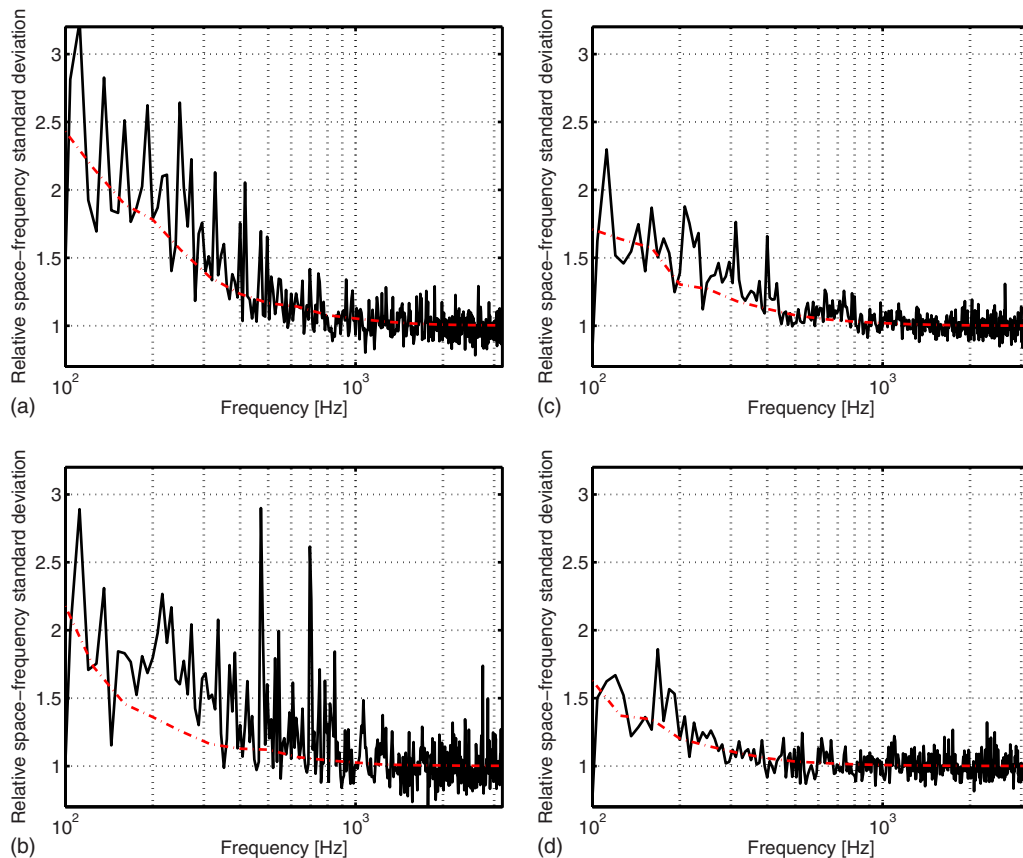


FIG. 2. (Color online) Relative space-frequency standard deviation of the mean-square value of one component of the particle velocity in (a) a small lightly damped room, (b) a small damped room, (c) a large reverberation room, and (d) a large damped reverberation room. Solid line: measured standard deviation; dash-dotted line: theory [Eq. (8)].

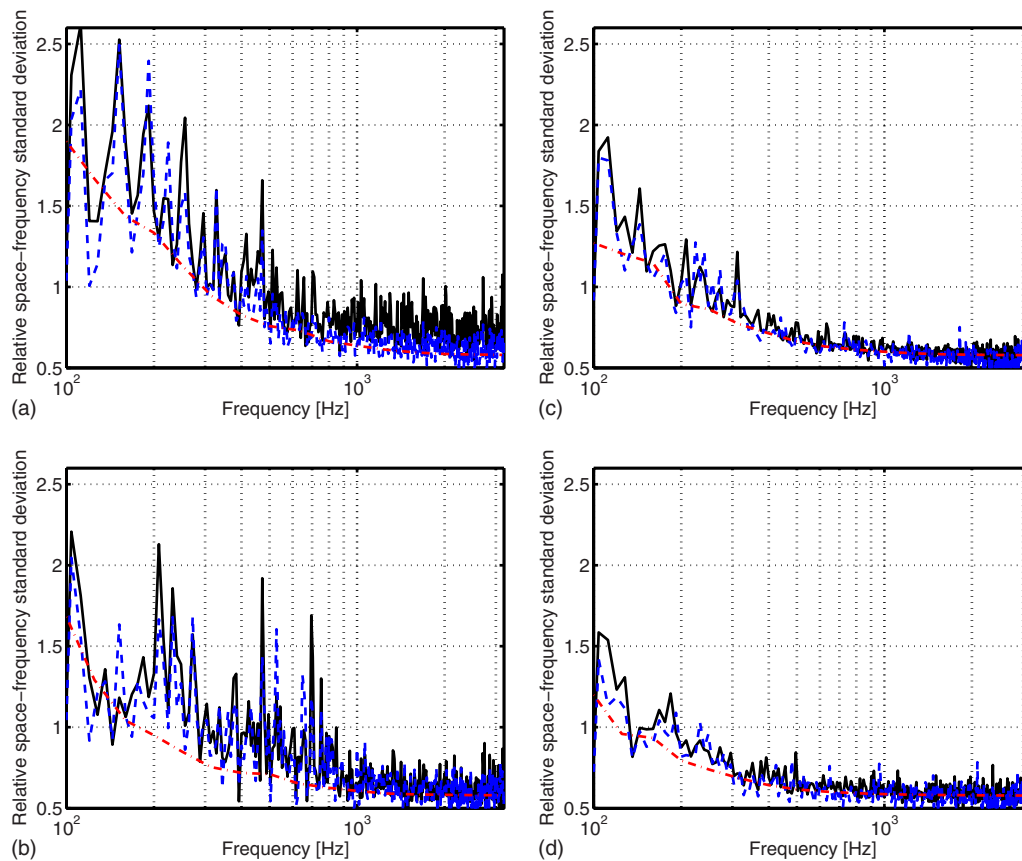


FIG. 3. (Color online) Relative space-frequency standard deviation of kinetic and total energy densities in (a) a small lightly damped room, (b) a small damped room, (c) a large reverberation room, and (d) a large damped reverberation room. Solid line: measured standard deviation of kinetic energy density; dashed line: measured standard deviation of total energy density; dash-dotted line: theory [Eqs. (10) and (12)].

has been described in detail in Ref. 14. Obviously one cannot measure in an ensemble of rooms, so in order to approach the full variation associated with ensemble statistics, both source and receiver positions were varied. In the postprocessing of the results, obtained at 25 pairs of positions, additional variations over 8 Hz bands (16 adjacent frequency bins) were also taken into account to produce space-frequency variations, which can be expected to approximate the ensemble variations.¹⁴

Figure 2 compares the measured relative space-frequency standard deviation of a single mean-square particle velocity component in an arbitrary direction with the predicted value calculated using Eq. (8). It is apparent that the results fluctuate significantly with frequency, but there is nevertheless fairly good agreement, confirming that a single mean-square particle velocity component exhibits the same statistics as the mean-square pressure. At high modal overlap the relative standard deviation approaches unity, but there is a large increase at low modal overlap. The agreement between measurements and predictions is better for the large room than for the small room, and for some reason Eq. (8) seems to underestimate the variations observed in the small damped room below the Schroeder frequency [Fig. 2(b)].

Figure 3 compares the relative space-frequency standard deviation of kinetic and total energy densities with the theory given by the identical expressions (10) and (12). The agreement is fairly good, confirming that the relative standard deviation of both quantities approaches $1/\sqrt{3} \approx 0.58$ at high

modal overlap and takes higher values at low modal overlap, although not as high values as the standard deviation of a single mean-square particle velocity component. In some cases the theory seems to underestimate the experimental results below the Schroeder frequency, though, but all data certainly confirm that the kinetic energy density exhibits the same statistics as the total energy density.

There is no obvious explanation for the tendency to underestimation observed in Fig. 2(b). The measurements presented in Fig. 3 are more difficult since they rely on accurate calibration of the three channels of the particle velocity transducer. Inaccurate calibration of the three channels of the particle velocity transducer may have emphasized one channel; this would tend to increase the experimental variance.

IV. NUMERICAL RESULTS

The full ensemble standard deviation is rather difficult to measure, but it can be estimated with a numerical model. A finite element model of 25 different rooms, constructed using the commercial software packet ACTRAN, was used in this investigation. The rooms were rectangular, and their dimensions were chosen as uniformly distributed random variables varying between 2 and 6 m. The source positions were placed randomly, but they were at least 0.4 m away from any wall. The calculations were carried out from 200 to 300 Hz with a frequency step of 2 Hz. The element size was chosen so as to provide a low numerical pollution in the examined

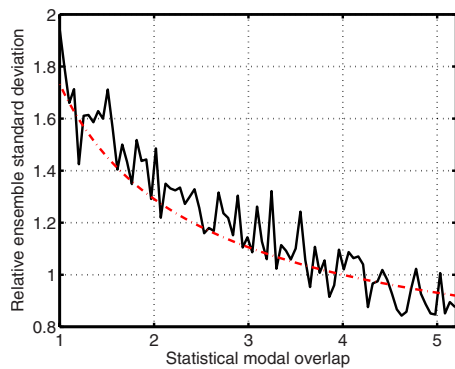


FIG. 4. (Color online) Relative ensemble standard deviation of kinetic energy density. Solid line: finite element calculations; dash-dotted line: theory [Eq. (10)].

frequency range. The mean-square values of the particle velocity vector were calculated at 50 000 randomly chosen nodal points of the mesh. Nodes closer than 0.4 m away from the walls or closer than 1 m from the source were not used. In order to determine the relative ensemble standard deviation as a function of the modal overlap, the data were sorted into appropriate modal overlap intervals. A similar technique was used recently in Refs. 14 and 15.

Figure 4 shows the results. There is excellent agreement, confirming the validity of Eq. (10) and indeed of the probabilistic approach described in Sec. II. Finally Fig. 5 compares the ratio of the relative variance of potential energy density to the relative variance of kinetic energy density with the theoretical ratio given by Eq. (11). There is very good agreement.

V. CONCLUSION

Waterhouse's simple free-wave theory has been extended to the region of low modal overlap and used for determining the relative ensemble variance of kinetic and total energy densities in reverberation rooms, and the predictions have been confirmed by experimental and numerical results. At high modal overlap, the relative variance of both quantities approaches one-third, and it is statistically three times

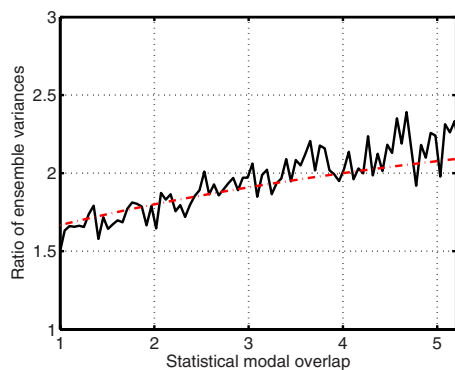


FIG. 5. (Color online) Ratio of relative variance of potential energy density to relative variance of kinetic energy density. Solid line: finite element calculations; dash-dotted line: theory [Eq. (11)].

more efficient to measure kinetic or total energy density than to measure potential energy density. At lower modal overlap, there is an increase in the relative variance of both kinetic and total energy densities that is inversely proportional to the modal overlap, that is, proportional to the ratio of the reverberation time to the room volume and inversely proportional to the square of the frequency. In this frequency range, the statistical advantage of measuring kinetic or total energy density is reduced, and ultimately halved, because the different components of the particle velocity are no longer statistically independent.

ACKNOWLEDGMENTS

The authors would like to thank Microflow for lending us a "USP" pressure-velocity transducer. F.J. would like to thank John Davy for suggesting approximating the ensemble variance by the space-frequency variance in the experiments.

- ¹R. V. Waterhouse and D. Lubman, "Discrete versus continuous space averaging in a reverberant sound field," *J. Acoust. Soc. Am.* **48**, 1–5 (1970).
- ²D. Lubman, R. V. Waterhouse, and C. Chien, "Effectiveness of continuous averaging in a diffuse sound field," *J. Acoust. Soc. Am.* **53**, 650–659 (1973).
- ³I. Wolff and F. Massa, "Direct measurement of sound energy density and sound energy flux in a complex sound field," *J. Acoust. Soc. Am.* **3**, 317–318 (1932).
- ⁴R. K. Cook and P. A. Schade, "New method for measurement of the total energy density of sound waves," in *Proceedings of the Inter-Noise 74*, Washington, DC (1974), pp. 101–106.
- ⁵F. Jacobsen, "The diffuse sound field," Ph.D. thesis, Technical University of Denmark, Kongens Lyngby, Denmark (1979).
- ⁶J. A. Moryl and E. L. Hixson, "A total acoustic energy density sensor with applications to energy density measurement in a reverberation room," in *Proceedings of the Inter-Noise 87*, Beijing, China (1987), pp. 1195–1198.
- ⁷J. W. Parkins, S. D. Sommerfeldt, and J. Tichy, "Error analysis of a practical energy density sensor," *J. Acoust. Soc. Am.* **108**, 211–222 (2000).
- ⁸B. S. Cazzolato and J. Ghan, "Frequency domain expressions for the estimation of time-averaged acoustic energy density," *J. Acoust. Soc. Am.* **117**, 3750–3756 (2005).
- ⁹J.-C. Pascal and J.-F. Li, "A systematic method to obtain 3D finite difference formulations for acoustic intensity and other energy quantities," *J. Sound Vib.* **310**, 1093–1111 (2008).
- ¹⁰F. Jacobsen, "A note on finite difference estimation of acoustic particle velocity," *J. Sound Vib.* **256**, 849–859 (2002).
- ¹¹D. R. Yntema, W. F. Druyvesteyn, and M. Elwenspoek, "A four particle velocity sensor device," *J. Acoust. Soc. Am.* **119**, 943–951 (2006).
- ¹²D. B. Nutter, T. W. Leishman, S. D. Sommerfeldt, and J. D. Blotter, "Measurement of sound power and absorption in reverberation chambers using energy density," *J. Acoust. Soc. Am.* **121**, 2700–2710 (2007).
- ¹³R. V. Waterhouse, "Statistical properties of reverberant sound fields," *J. Acoust. Soc. Am.* **43**, 1436–1444 (1968).
- ¹⁴F. Jacobsen and A. Rodríguez Molaes, "Sound power emitted by a pure-tone source in a reverberation room," *J. Acoust. Soc. Am.* **126**, 676–684 (2009).
- ¹⁵F. Jacobsen and A. Rodríguez Molaes, "The ensemble variance of pure-tone measurements in reverberation rooms," *J. Acoust. Soc. Am.* **127**, 233–237 (2010).
- ¹⁶A. Papoulis and S. U. Pillai, *Probability, Random Variables, and Stochastic Processes*, 4th ed. (McGraw-Hill, New York, 1991).
- ¹⁷R. L. Weaver and J. Burkhardt, "Weak Anderson localization and enhanced backscatter in reverberation rooms and quantum dots," *J. Acoust. Soc. Am.* **96**, 3186–3190 (1994).
- ¹⁸J. L. Davy, "The variance of the discrete frequency transmission function of a reverberation room," *J. Acoust. Soc. Am.* **126**, 1199–1206 (2009).
- ¹⁹F. Jacobsen and V. Jaud, "A note on the calibration of pressure-velocity sound intensity probes," *J. Acoust. Soc. Am.* **120**, 830–837 (2006).